Optik - International Journal for Light and Electron Optics 245 (2021) 167669

Contents lists available at ScienceDirect

Optik

journal homepage: www.elsevier.com/locate/ijleo

Original research article

Polarization-insensitive dual-band terahertz metamaterial absorber based on asymmetric arrangement of two rectangular-shaped resonators

Dac Tuyen Le [a,*], Ba Tuan Tong [a], Thi Kim Thu Nguyen [b], Thanh Nghia Cao [b], Hong Quang Nguyen [b], Manh Cuong Tran [c], Chi Lam Truong [d], Xuan Khuyen Bui [e], Dinh Lam Vu [f], Thi Quynh Hoa Nguyen [b,*]

[a] Department of Physics, Hanoi University of Mining and Geology, 18 Pho Vien, Hanoi, Vietnam
[b] School of Engineering and Technology, Vinh University, 182 Le Duan, Vinh City, Vietnam
[c] Faculty of Physics, Hanoi National University of Education, 136 Xuan Thuy, Hanoi, Vietnam
[d] NTT Hi-Tech Institute, Nguyen Tat Thanh University, 300A Nguyen Tat Thanh, Ho Chi Minh City, Vietnam
[e] Institute of Materials Science, Vietnam Academy of Science and Technology, 18 Hoang Quoc Viet, Hanoi, Vietnam
[f] Graduate University of Science and Technology, Vietnam Academy of Science and Technology, 18 Hoang Quoc Viet, Hanoi, Vietnam

ARTICLE INFO

Keywords:
Metamaterials
Dual-band THz absorber
Polarization-insensitive absorber

ABSTRACT

We present a design of a polarization-insensitive dual-band metamaterial absorber (MA) in the THz region by employing a three-layer structure consisting of a rectangular-shaped resonator on top of silicon and metallic film. Finite-difference time domain (FDTD) simulation indicates that two perfect absorption peaks can be achieved at 5.35 and 9.0 THz with absorptivity greater than 96% under normal incidence. The asymmetry in design structure eliminates any polarization dependence, and absorptivity is nearly 80% for large incidence angle up to 60°. The individual absorption band can be tuned by varying the dimensions of the rectangular-shaped resonator. The design idea provides a new strategy to achieve polarization-insensitive MA by arranging structure and can be extended to other bands.

1. Introduction

Metamaterial (MM) is an artificial structure that is engineered to achieve the desirable electromagnetic (EM) properties not available in naturally occurring materials [1,2]. In the past decade, there have been many reports on fantastic EM phenomena of MM, such as negative refraction, superlens, camouflage [1–4]. By employing the resonance characteristics and limited field enhancement effects, MM has been applied in imaging, sensing, filter, polarizer, and absorber [5–11]. As one of the important functional devices, metamaterial absorber (MA) has become a major research focus in the fields of MM since the first experimental demonstration was developed by Landy et al. [9]. The absorption mechanism has been explained by several methods such as effective medium, electric and/or magnetic resonance, interference theory, plasmon resonance, electromagnetically-induced transparency (EIT), and plasmon-induced transparency (PIT) [9–18]. Normally, MAs consist of three layers: the periodic structure as frequency selective resonator, a dielectric spacer layer, and a metallic film as blocking transmission waves. Based on this configuration, MAs were widely

* Corresponding authors.
E-mail addresses: ledactuyen@humg.edu.vn (D.T. Le), ntqhoa@vinhuni.edu.vn (T.Q.H. Nguyen).

https://doi.org/10.1016/j.ijleo.2021.167669
Received 23 February 2021; Received in revised form 17 July 2021; Accepted 17 July 2021
Available online 21 July 2021

studied from radio frequency range to optical frequencies [9–32]. Recently, various MA structures for THz frequencies have been proposed and investigated intensively from narrow to multi-band or broadband [23–32]. However, the design of MA with high absorption characteristics including incident-angle stability and polarization insensitivity remains challenging [33–36]. The turning of the resonator dimensions is used to control the working frequency range. Meanwhile, the polarization insensitivity can be realized by designing the absorber with symmetry structures such as circle, square, ring, and cross which exhibit a single absorption band due to these resonant features [37–40]. Therefore, to design multi-band or broadband THz MA, integrating multiple symmetry resonators have been developed [41–43], which would be relatively complex to fabricate. Another approach to obtain multi-band absorption, the design of MA is based on an asymmetry structure [30–32]. However, the main drawback of this approach is polarization sensitivity so that the asymmetry structures exhibit a low value of absorption due to consideration of cross-polarized reflections [44–46]. Ghobadi et. al. reported an optimum unit cell arrangement in a metal-insulator-metal (MIM) based ultra-broadband absorber to achieve near-perfect polarization-independent that regardless of the shape of the resonator [47]. Zhang et al. proposed a dual-band absorber that showed the polarization insensitivity by carefully arranging an elliptical nanodisk array [48].

In this study, we propose a dual-band terahertz MA based on an arrangement of two rectangular-shaped resonators in a two-dimensionally asymmetric structure. The design exhibits multiple advantages over other asymmetric structures such as simple reconfigurability, high absorption efficiency, polarization independence, and incident angle insensitivity. With excellent performance, our design structure can provide a useful approach to realize THz devices.

2. Design and simulation

Fig. 1 illustrates the font view and three-dimensional structure of the proposed MA with a periodicity of $P = 16$ μm. Our design is a three-layer structure consisting of a silicon layer sandwiched between two metallic layers. Gold is chosen to use at the metallic layers because it is strong and resistant to atmospheric oxidation. We eliminated the polarization sensitivity by arranging two rectangular-shaped gold stripes that are perpendicular to each other in a two-dimensionally asymmetric structure. The length and width of the rectangle are $a = 8$ μm and $b = 4$ μm, respectively. The rectangles are located from the center of the unit cell at $c = 2$ μm and $d = 3$ μm. The back layer is a continuous plate covering the whole side. The thickness and electric conductivity of the gold layers are $t = 0.1$ μm and $\sigma = 4.56 \times 10^7$ S/m, respectively. The silicon has a dielectric constant of 11.9, a loss tangent of 0.015, and a thickness (h) of 1 μm. The design parameters (a and b) can be varied to investigate the controllability of the absorption properties of the proposed MA.

To evaluate the absorption performance, the simulation method is performed using finite-difference time domain (FDTD) solver - CST Microwave Studio [49]. In this study, perfectly matched layers are applied along the z-direction and periodic boundary conditions in the x-and y-directions. As given in Fig. 1(a), the periodic structure is illuminated by an incident plane wave with the electric field parallel to the x-axis. The polarization angle φ is the angle between the E-direction (H-direction) and the x-axis (y-axis). When the E-direction is parallel to the x-axis, the polarization angle is zero. Since the gold plate blocked transmission, the absorption is calculated by $A = 1 - |S_{11}|^2$, where $|S_{11}|^2 = R$ is reflection.

3. Results and discussion

Fig. 2 shows the absorption spectra of the proposed MA with various arrangements of the rectangular-shaped resonator at normal incidence with two polarization angles of 0° and 90°. As shown in Fig. 2(a) and (b) for the polarization angle of 0°, when the individual rectangle is at the center of the unit cell, the vertical or horizontal strips exhibit a single perfect absorption peak at 5.35 THz or 9.0 THz, respectively (black lines). Meanwhile, for the polarization angle of 90°, the absorption peak is respectively inverted to 9.0 THz and 5.35 THz (red lines). It is reasonable that the geometrical symmetry of the vertical and horizontal rectangles have inverted each other. The obtained results indicate that the individual vertical and horizontal rectangular-shaped resonator exhibits polarization-sensitive absorption due to its asymmetry structure. However, by combining both vertical and horizontal rectangular-shaped resonators as shown in Fig. 2(c), we can obtain two absorption peaks of 5.35 THz and 9.0 THz, corresponding to the absorptivity of 97.6% and 96.9%, respectively. Furthermore, these absorption peaks are unchanged with different polarization angles of 0° and 90°.

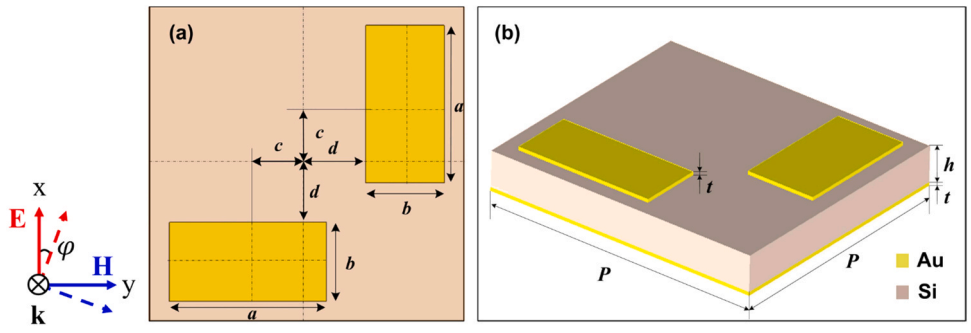

Fig. 1. Schematic diagram of the proposed MA with structural parameter and incident electromagnetic wave: (a) front view and (b) three-dimensional structure.

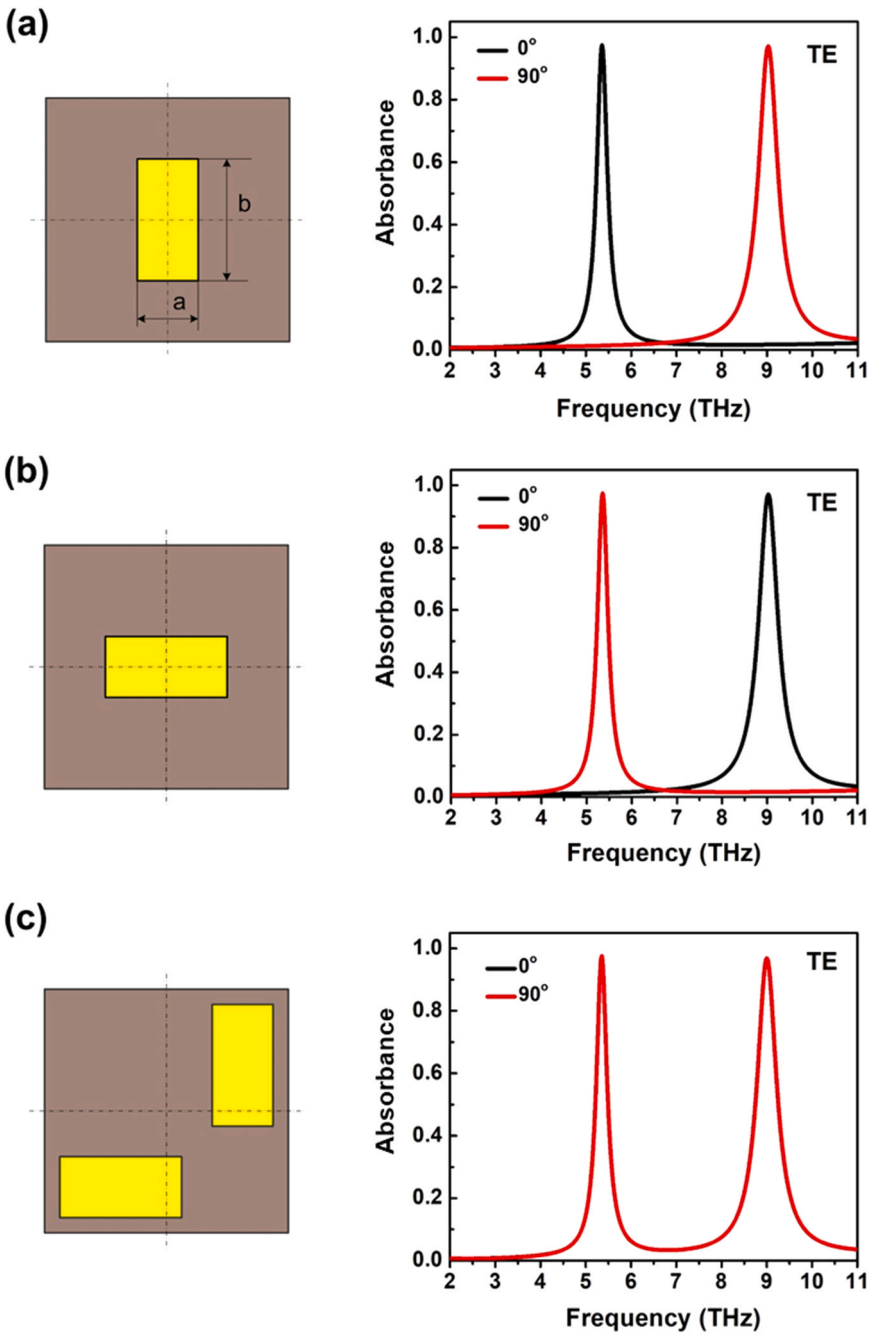

Fig. 2. Absorption spectra of the proposed MA with various arrangements of the rectangular-shaped resonator at normal incidence with two polarization angles of 0° and 90°.

To further evaluate the absorption performance, the dependence of absorption spectra on the different polarization angles under both TE and TM waves is shown in Fig. 3. The peak position and absorptivity are stable when polarization angles are varied from 0° to 90°. It indicates that the proposed MA exhibits polarization-insensitive absorption property. These results also confirm that polarization insensitivity can be achieved by arranging an asymmetry structure.

Furthermore, the dependence of absorption spectra on incident angles is also investigated as shown in Fig. 4. For both TE and TM waves, the absorption spectra of the proposed MA are virtually unchanged with incident angles from 0° to 30°. For the incident angle of 60°, the absorptivity at two frequencies 5.35 THz and 9.0 THz is greater than 77.8% and 92.2% for TE waves, and 99.0% and 82.3% for TM waves, respectively. At the incident angle of 70°, these values can still maintain greater than 60% for both TE and TM waves. By arranging both vertical and horizontal rectangular-shaped resonators, the absorption spectra of the proposed MA are not only

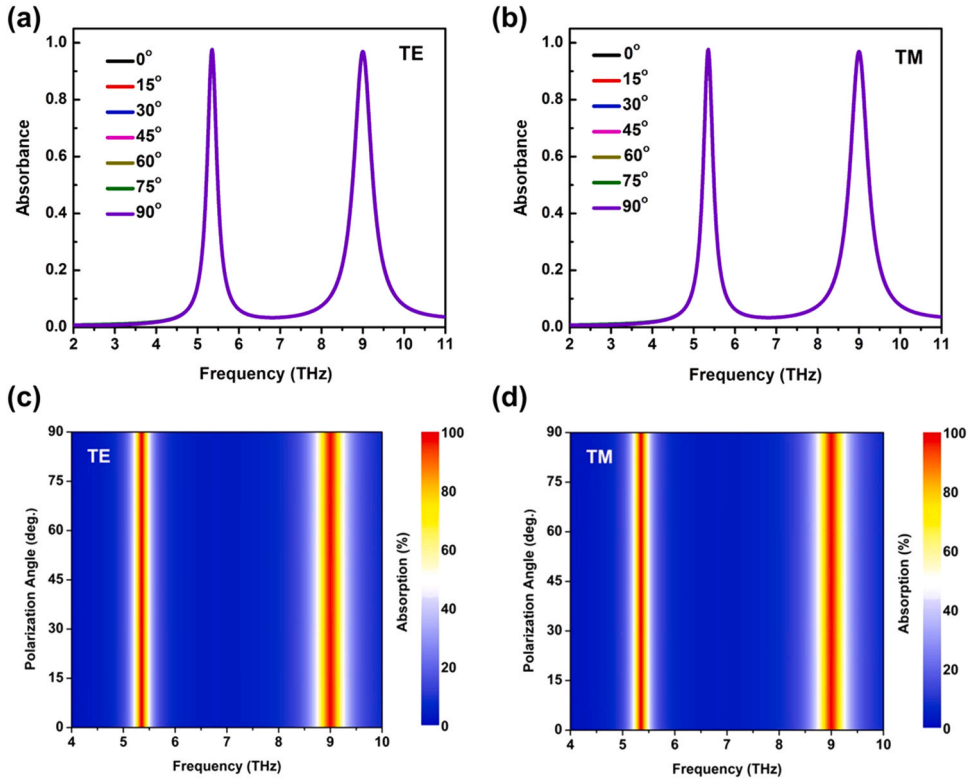

Fig. 3. The dependence of absorption spectra on polarization angle for (a, c) TE and (b, d) TM polarizations.

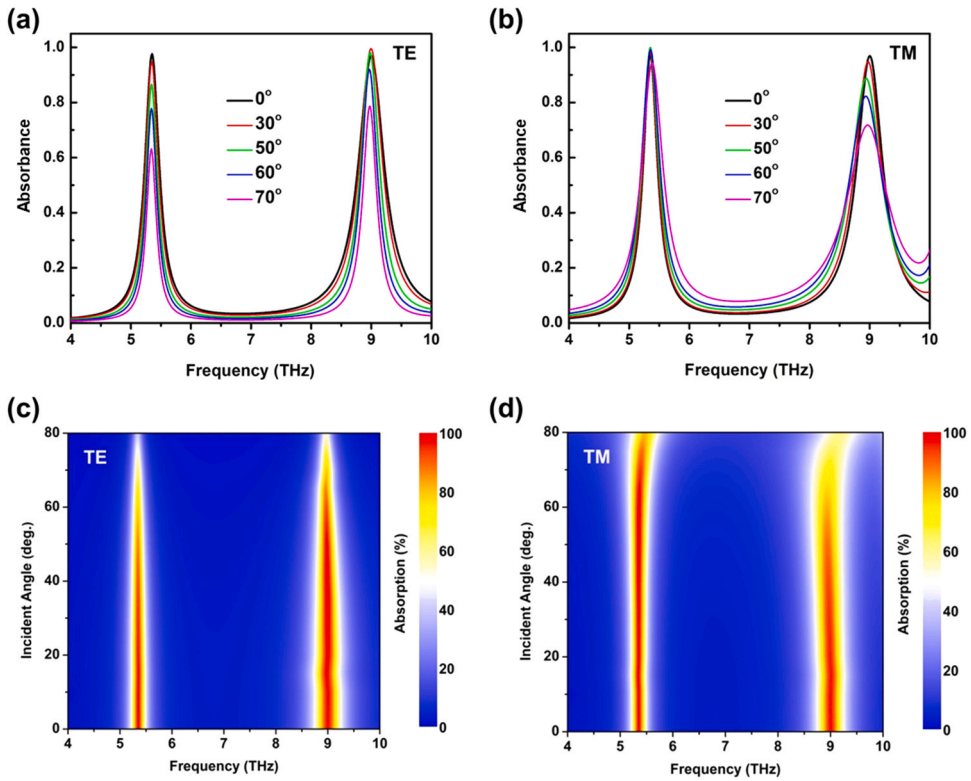

Fig. 4. The dependence of absorption spectra on the incident angle for (a, c) TE and (b, d) TM waves.

polarization independence but also incident angle insensitivity.

To achieve the perfect absorption, the impedance matching between the free space and the proposed MA at the resonant frequency must be satisfied. The normalized input impedance (Z) of the MA can be calculated based on the effective medium interference theory given by Eq. (1) [46,50].

$$Z = \sqrt{\frac{(1+S_{11})^2 - {S_{21}}^2}{(1-S_{11})^2 - {S_{21}}^2}} = \frac{1+S_{11}}{1-S_{11}} \tag{1}$$

As seen in Fig. 5, at the resonant frequencies of 5.35 THz and 9.0 THz, the real part and the imaginary part of the normalized impedance are approximately 1 and 0, respectively, indicating the impedance matching occurred in the proposed MA structure.

The absorption mechanism is related to the electric dipolar resonance in the rectangular-shaped resonator due to localized surface plasmon resonance and magnetic resonance. Fig. 6 presents the electric field distribution at two absorption peaks. The electric field is mainly concentrated at the upper and lower edges of the vertical and horizontal strips according to resonant frequencies of 5.35 THz and 9.0 THz, respectively. It indicates that the charge distribution is accumulated on the upper and lower edges of the rectangular-shaped resonator.

Furthermore, the current distribution in the rectangular-shaped resonator and the back layer at 5.35 THz and 9.0 THz is shown in Fig. 7. The anti-parallel currents are formed on the gold rectangle and the back gold mirror which creates circulating currents between the two gold layers. This circulating current is known as a magnetic resonance in which an induced magnetic moment strongly interacts with the incident magnetic field [9,11,51]. Therefore, strong enhancement of the localized electromagnetic field is excited between front and back layers at the resonant frequencies.

We further investigate the dual-band absorber by changing the lengths (a) and width (b) of the gold rectangle that enables a change in the absorption peaks. Fig. 8(a) shows the absorption spectra with tunable lengths of the gold rectangle without optimizing other parameters. The absorptivity remains higher than 96% at both resonant frequencies. Increasing the length of the gold rectangle from 6.8 μm to 9.2 μm causes a red-shift of the lower resonant frequency from 6.68 THz to 4.7 THz while the higher one is maintained. It confirms that the lower resonant frequency is mainly related to the length of the rectangular-shaped resonator. The red-shift of the absorption peak can be explained by the plasmonic resonance with the increasing size of the resonator. In addition, the red-shift is associated with the equivalent LC circuit in which the resonant frequency is determined by $f = 1/(2\pi\sqrt{LC})$, and the inductance L is proportional to the size of length [11,51,52]. Similar, when the width of the gold rectangle is increasing from 2.8 μm to 5.2 μm, the higher resonant frequency is also a red-shift from 11.6 THz to 7.3 THz while the lower one exhibits a tiny change as shown in Fig. 8(b). It also confirms the higher resonant frequency associates with the width of the rectangular-shaped resonator. The results indicate that the two absorption bands can also be adjusted individually and the great flexibility of our dual-band MA over in the THz region.

4. Conclusion

We demonstrate a dual-band absorption in the THz region by utilizing an asymmetric arrangement of a rectangular-shaped resonator. The absorption peaks are obtained at the resonant frequencies of 5.35 THz and 9.0 THz with the absorptivity greater than 96% and polarization-insensitive under normal incidence, and the absorptivity of nearly 80% is maintained with incidence angle up to 60° for both TE and TM waves. Interestingly, the individual absorption band is tunable by varying the dimensions of the gold rectangle. With its excellent performance, our design structure can be valuable in many applications such as imaging and sensing and readily extended to other frequency ranges.

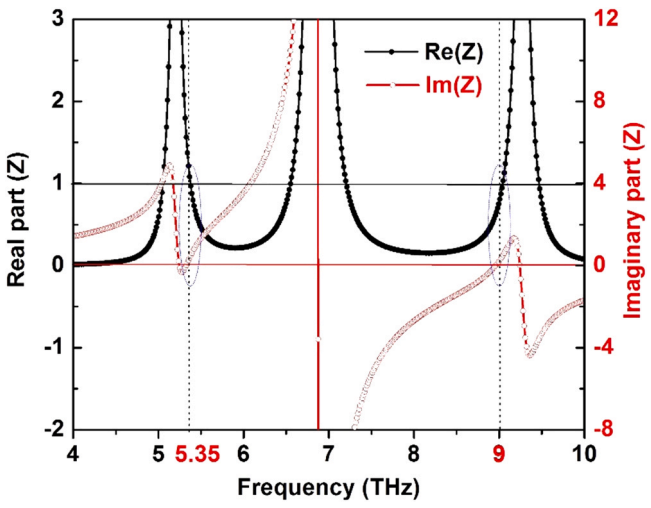

Fig. 5. The extracted effective impedance (Z) of the proposed MA under normal incidence.

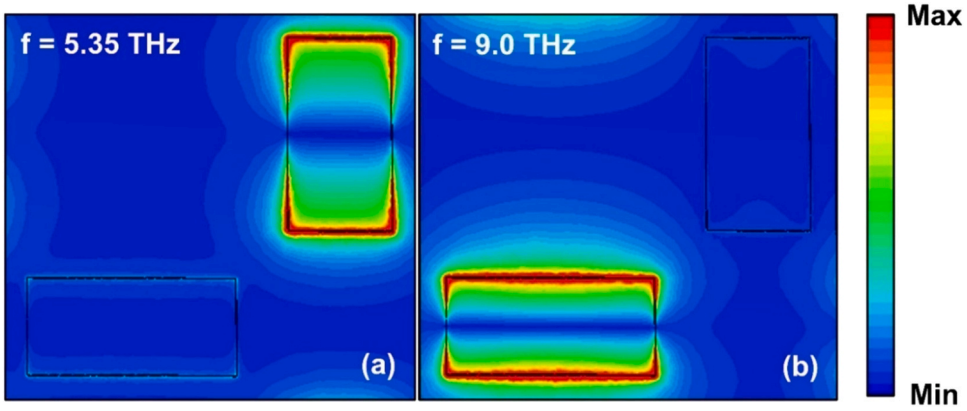

Fig. 6. Electric field distribution of the proposed MA under normal incidence for TE polarization at (a) 5.35 THz and (b) 9.0 THz.

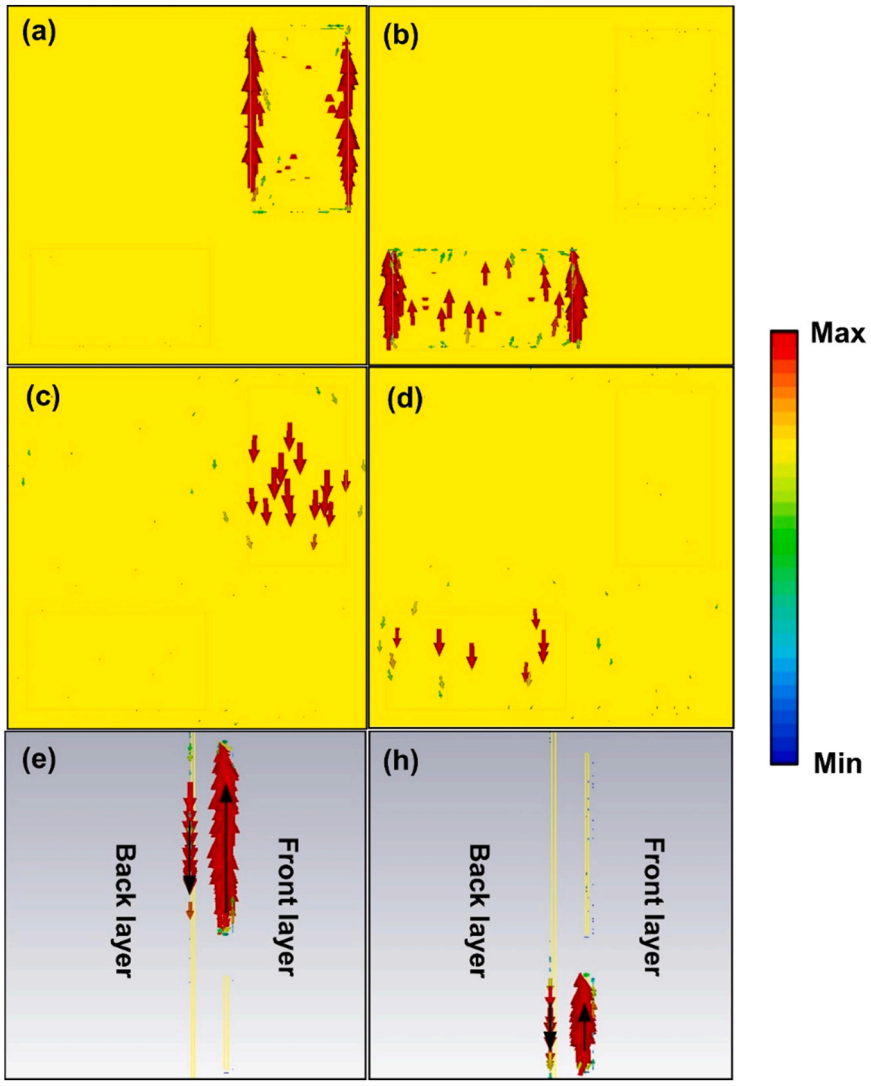

Fig. 7. Current distributions on (a, b) the front layer, (c, d) the back layers, and (e, f) the cross-section of xoz plane under normal incidence for TE polarization at the resonant frequencies of (a, c, e) 5.35 THz and (b, d, h) 9.0 THz, respectively.

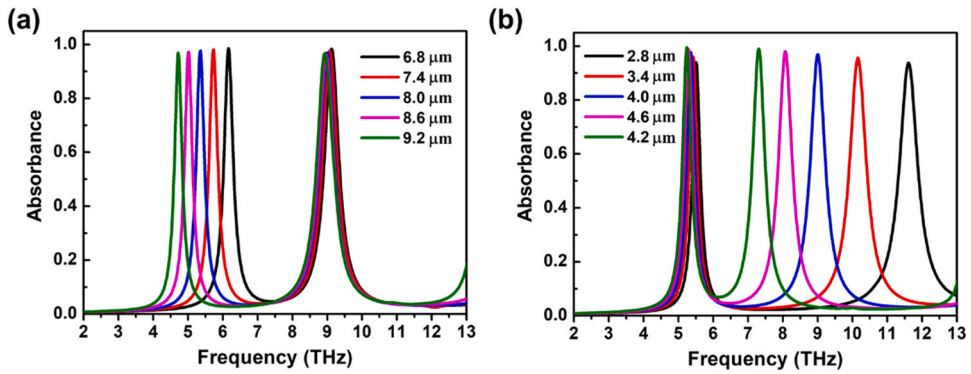

Fig. 8. Absorption spectra of the proposed MA with various lengths and widths of the rectangular resonator (a) length and (b) width under normal incidence for TE polarization.

Declaration of Competing Interest

The authors declare that they have no known competing financial interests or personal relationships that could have appeared to influence the work reported in this paper.

Acknowledgements

This research is supported by Vietnam National Foundation for Science and Technology Development (NAFOSTED) (grant number 103.99-2020.45) and Ministry of Education and Training, Vietnam (grant number B2020-MDA-10).

References

[1] D.R. Smith, W.J. Padilla, D.C. Vier, S.C. Nemat-Nasser, S. Schultz, Composite medium with simultaneously negative permeability and permittivity, Phys. Rev. Lett. 84 (2000) 4184–4187.
[2] K. Fan, W.J. Padilla, Dynamic electromagnetic metamaterials, Mater. Today 18 (2015) 39–50.
[3] N. Fang, H. Lee, C. Sun, X. Zhang, Sub-diffraction-limited optical imaging with a silver superlens, Science 308 (5721) (2005) 534–537.
[4] D. Schurig, J.J. Mock, B.J. Justice, S.A. Cummer, J.B. Pendry, A.F. Starr, D.R. Smith, Metamaterial electromagnetic cloak at microwave frequencies, Science 314 (5801) (2006) 977–980.
[5] S. Haxha, F. AbdelMalek, F. Ouerghi, M. Charlton, A. Aggoun, X. Fang, Metamaterial superlenses operating at visible wavelength for imaging applications, Sci. Rep. 8 (2018) 16119.
[6] A. Lochbaum, A. Dorodnyy, U. Koch, S.M. Koepfli, S. Volk, Y. Fedoryshyn, V. Wood, J. Leuthold, Compact mid-infrared gas sensing enabled by an all-metamaterial design, Nano Lett. 20 (6) (2020) 4169–4176.
[7] W. Yang, Y.S. Lin, Tunable metamaterial filter for optical communication in the terahertz frequency range, Opt. Express 28 (2020) 17620–17629.
[8] T.K.T. Nguyen, T.M. Nguyen, H.Q. Nguyen, T.N. Cao, D.T. Le, X.K. Bui, S.T. Bui, C.L. Truong, D.L. Vu, T. Nguyen, Simple design of efficient broadband multifunctional polarization converter for X-band applications, Sci. Rep. 11 (2021) 2032.
[9] N.I. Landy, S. Sajuyigbe, J.J. Mock, D.R. Smith, W.J. Padilla, Perfect metamaterial absorber, Phys. Rev. Lett. 100 (2008), 207402.
[10] P. Yu, L.V. Besteiro, Y. Huang, J. Wu, L. Fu, H.H. Tan, C. Jagadish, G.P. Wiederrecht, A.O. Govorov, Z. Wang, Broadband metamaterial absorbers, Adv. Opt. Mater. 7 (2019), 1800995.
[11] D.T. Viet, N.T. Hien, P.V. Tuong, N.Q. Minh, P.T. Trang, L.N. Le, Y.P. Lee, V.D. Lam, Perfect absorber metamaterials: peak, multi-peak and broadband absorption, Opt. Commun. 322 (2014) 209–213.
[12] Hou-Tong Chen, Interference theory of metamaterial perfect absorbers, Opt. Express 20 (2012) 7165–7172.
[13] H. Zhu, F. Yi, E. Cubukcu, Plasmonic metamaterial absorber for broadband manipulation of mechanical resonances, Nat. Photon 10 (2016) 709–714.
[14] D.C. Zografopoulos, M. Swillam, R. Beccherelli, Hybrid plasmonic modulators and filters based on electromagnetically induced transparency, IEEE Photonics Technol. Lett. 28 (2016) 818–821.
[15] C. Wang, X. Jiang, G. Zhao, M. Zhang, C.W. Hsu, B. Peng, A.D. Stone, L. Jiang, L. Yang, Electromagnetically induced transparency at a chiral exceptional point, Nat. Phys. 16 (2020) 334–340.
[16] B. Gerislioglu, A. Ahmadivand, N. Pala, Tunable plasmonic toroidal terahertz metamodulator, Phys. Rev. B 97 (2018), 161405.
[17] M.A. Baqir, P.K. Choudhury, A. Farmani, et al., Tunable plasmon induced transparency in graphene and hyperbolic metamaterial-based structure, IEEE Photonics J. 11 (2019), 4601510.
[18] R.M.H. Bilal, M.A. Baqir, P.K. Choudhury, M.M. Ali, A.A. Rahim, Tunable and multiple plasmon-induced transparency in a metasurface comprised of silver s-shaped resonator and rectangular strip, IEEE Photonics J. 12 (2020), 4500913.
[19] K.H. Fung, J. Xu, H. Ma, Y. Jin, S. He, N.X. Fang, Ultrabroadband light absorption by a sawtooth anisotropic metamaterial slab, Nano Lett. 12 (3) (2012) 1443–1447.
[20] L.D. Hai, V.D. Qui, N.H. Tung, T.V. Huynh, N.D. Dung, N.T. Binh, L.D. Tuyen, V.D. Lam, Conductive polymer for ultra-broadband, wide-angle, and polarization-insensitive metamaterial perfect absorber, Opt. Express 26 (2018) 33253–33262.
[21] M.C. Tran, V.H. Pham, T.H. Ho, T.T. Nguyen, H.T. Do, X.K. Bui, S.T. Bui, D.T. Le, T.L. Pham, D.L. Vu, Broadband microwave coding metamaterial absorbers, Sci. Rep. 10 (2020) 1810.
[22] D. Wu, C. Liu, Y. Liu, L. Yu, Z. Yu, L. Chen, R. Ma, H. Ye, Numerical study of an ultra-broadband near-perfect solar absorber in the visible and near-infrared region, Opt. Lett. 42 (2017) 450–453.
[23] H. Liu, Z.H. Wang, L. Li, Y.X. Fan, Z.Y. Tao, Vanadium dioxide-assisted broadband tunable terahertz metamaterial absorber, Sci. Rep. 9 (2019) 5751.
[24] D. Yang, C. Zhang, X. Ju, Y. Ji, C. Lan, Multi-resonance and ultra-wideband terahertz metasurface absorber based on micro-template-assisted self-assembly method, Opt. Express 28 (2020) 2547–2556.
[25] Y. He, Q. Wu, S. Yan, Multi-band terahertz absorber at 0.1–1 THz frequency based on ultra-thin metamaterial, Plasmonics 14 (2019) 1303–1310.

[26] C. Gong, M. Zhan, J. Yang, Z. Wang, H. Liu, Y. Zhao, W. Liu, Broadband terahertz metamaterial absorber based on sectional asymmetric structures, Sci. Rep. 6 (2016) 32466.
[27] M. Janneh, A.D. Marcellis, E. Palange, A.T. Tenggara, D. Byun, Design of a metasurface-based dual-band Terahertz perfect absorber with very high Q-factors for sensing applications, Opt. Commun. 416 (2018) 152–159.
[28] X. Chen, W. Fan, Ultra-flexible polarization-insensitive multiband terahertz metamaterial absorber, Appl. Opt. 54 (2015) 2376–2382.
[29] Y. Ma, Q. Chen, J. Grant, S.C. Saha, A. Khalid, D.R.S. Cumming, A terahertz polarization insensitive dual band metamaterial absorber, Opt. Lett. 36 (2011) 945–947.
[30] W. Xin, Z. Binzhen, W. Wanjun, W. Junlin, D. Junping, Design, fabrication, and characterization of a flexible dual-band metamaterial absorber, IEEE Photonics J. 9 (2017), 4600512.
[31] T. Lu, D. Zhang, P. Qiu, J. Lian, M. Jing, B. Yu, J. Wen, S. Zhuang, Dual-band perfect metamaterial absorber based on an asymmetric H-shaped structure for terahertz waves, Materials 11 (2018) 2193.
[32] Y. Bai, L. Zhao, D. Ju, Y. Jiang, L. Liu, Wide-angle, polarization-independent and dual-band infrared perfect absorber based on L-shaped metamaterial, Opt. Express 23 (2015) 8670–8680.
[33] T.Q.H. Nguyen, T.K.T. Nguyen, T.N. Cao, H. Nguyen, L.G. Bach, Numerical study of a broadband metamaterial absorber using a single split circle ring and lumped resistors for X-band applications, AIP Adv. 10 (2020), 035326.
[34] T.T. Nguyen, S. Lim, Wide incidence angle-insensitive metamaterial absorber for both TE and TM polarization using eight-circular-sector, Sci. Rep. 7 (2017) 3204.
[35] T.T. Nguyen, S. Lim, Angle- and polarization-insensitive broadband metamaterial absorber using resistive fan-shaped resonators, Appl. Phys. Lett. 112 (2018), 021605.
[36] N.T.Q. Hoa, P.D. Tung, N.D. Dung, H. Nguyen, T.S. Tuan, Numerical study of a wide incident angle- and polarisation-insensitive microwave metamaterial absorber based on a symmetric flower structure, AIP Adv. 9 (2019), 065318.
[37] Y. Lu, J. Li, S. Zhang, J. Sun, J.Q. Yao, Polarization-insensitive broadband terahertz metamaterial absorber based on hybrid structures, Appl. Opt. 57 (2018) 6269–6275.
[38] R.M.H. Bilal, M.A. Baqir, P.K. Choudhury, M.M. Ali, A.A. Rahim, W. Kamal, Polarization-insensitive multi-band metamaterial absorber operating in the 5G spectrum, Optik 216 (2020), 164958.
[39] H. Tao, N.I. Landy, C.M. Bingham, X. Zhang, R.D. Averitt, W.J. Padilla, A metamaterial absorber for the terahertz regime: design, fabrication and characterization, Opt. Express 16 (2008) 7181–7188.
[40] J. Grant, Y. Ma, S. Saha, L.B. Lok, A. Khalid, D.R.S. Cumming, Polarization insensitive terahertz metamaterial absorber, Opt. Lett. 36 (2011) 1524–1526.
[41] H. Pan, H. Zhang, X. Tian, D. Zhang, Design, simulation, and analysis of an ultra-broadband polarization-insensitive terahertz metamaterial absorber, J. Opt. Soc. Am. B 38 (2021) 95–103.
[42] B.X. Wang, Y. He, P. Lou, W. Xing, Design of a dual-band terahertz metamaterial absorber using two identical square patches for sensing application, Nanoscale Adv. 2 (2020) 763–769.
[43] X. Du, F. Yan, W. Wang, S. Tan, L. Zhang, Z. Bai, H. Zhou, Y. Hou, A polarization- and angle-insensitive broadband tunable metamaterial absorber using patterned graphene resonators in the terahertz band, Opt. Laser Technol. 132 (2020), 106513.
[44] T. Beeharry, R. Yahiaoui, K. Selemani, H.H. Ouslimani, A co-polarization broadband radar absorber for RCS reduction, Materials 11 (2018) 1668.
[45] J. Xu, R. Li, S. Wang, T. Han, Ultra-broadband linear polarization converter based on anisotropic metasurface, Opt. Express 26 (2018) 26235–26241.
[46] T.S. Tuan, V.D. Lam, N.T.Q. Hoa, Simple design of a copolarization wideband metamaterial absorber for C-band applications, J. Electron. Mater. 48 (2019) 5018–5027.
[47] A. Ghobadi, H. Hajian, M. Gokbayrak, S.A. Dereshgi, A. Toprak, B. Butun, E. Ozbay, Visible light nearly perfect absorber: an optimum unit cell arrangement for near absolute polarization insensitivity, Opt. Express 25 (2017) 27624–27634.
[48] B. Zhang, Y. Zhao, Q. Hao, B. Kiraly, I.C. Khoo, S. Chen, T.J. Huang, Polarization-independent dual-band infrared perfect absorber based on a metal-dielectric-metal elliptical nanodisk array, Opt. Express 19 (2011) 15221–15228.
[49] ⟨https://www.3ds.com/products-services/simulia/products/cst-studio-suite/⟩.
[50] D.R. Smith, D.C. Vier, T. Koschny, C.M. Soukoulis, Electromagnetic parameter retrieval from in homogeneous metamaterials, Phys. Rev. E 71 (2005), 036617.
[51] J. Zhou, E.N. Economon, T. Koschny, C.M. Soukoulis, Unifying approach to left-handed material design, Opt. Lett. 31 (2006) 3620–3622.
[52] A. Sellier, T.V. Teperik, A. de Lustrac, Resonant circuit model for efficient metamaterial absorber, Opt. Express 21 (2013) A997–A1006.